

Quantum aspects of brain activity and the role of consciousness

FRIEDRICH BECK* AND JOHN C. ECCLES†

*Institut für Kernphysik, Technische Hochschule Darmstadt, D-6100 Darmstadt, Germany; and †Max-Planck-Institut für Hirnforschung, D-6000 Frankfurt a.M. 71, Germany

Contributed by John C. Eccles, July 21, 1992

ABSTRACT The relationship of brain activity to conscious intentions is considered on the basis of the functional microstructure of the cerebral cortex. Each incoming nerve impulse causes the emission of transmitter molecules by the process of exocytosis. Since exocytosis is a quantal phenomenon of the presynaptic vesicular grid with a probability much less than 1, we present a quantum mechanical model for it based on a tunneling process of the trigger mechanism. Consciousness manifests itself in mental intentions. The consequent voluntary actions become effective by momentary increases of the probability of vesicular emission in the thousands of synapses on each pyramidal cell by quantal selection.

There has been an increasing interest in the relations of quantum mechanics, brain activities, and consciousness (1–4). On the part of quantum physics the impetus came from the interpretation of the measuring process, which is still on debate, even after more than 60 years of overwhelmingly successful applications of quantum theory. However, there is the question from neuroscience (5) whether quantum action is needed to understand the functioning of the brain in its subtle relations to experience, memory, and consciousness.

It was Wigner (6), in his stringent analysis of the consequences of measurements in a Stern–Gerlach experiment, who first speculated that the von Neumann collapse of the wave function (7) actually occurs by an act of consciousness in the human brain and is not describable in terms of ordinary quantum mechanics. More recently similar ideas were put forward and partly combined with Everett's "many-world" interpretation (8) of quantum theory (2). Other authors (e.g., ref. 1) have related quantum theory to consciousness on the basis of the usual interpretation of the state vector as a superposition of actualities [or "propensities," in Popper's nomenclature (9)]. Not much connection has been made, however, to the empirically established facts of brain physiology, nor have those authors attempted to locate a quantal process in the functional microsites of the neocortex.

In this work we contribute to filling this gap by putting forward a quantum mechanical description of bouton exocytosis. The next section gives an outline of the structure and activity of the neocortex as introduction to the quantum mechanical model. This is set up in the subsequent section. Finally, the hypothesis for a coherent coupling of the individual probability amplitudes is introduced. In this model action becomes possible by influence of a conscious will.

Neocortical Activity

Fig. 1A illustrates the universally accepted six laminae of the neocortex (10) with two large pyramidal cells in lamina V, three in lamina III, and two in lamina II. The pyramidal apical dendrites finish in a tuft-like branching in lamina I (Fig. 2A). There is agreement by Peters and Fleischhauer and their associates (12, 13) that the apical bundles or clusters dia-

grammatically shown in Fig. 2B are the basic anatomical units of the neocortex. They are observed in all areas of the cortex that have been investigated and in all mammals, including humans[‡]. It has been proposed that these bundles are the cortical units for reception (5), which would give them a preeminent role. Since they are composed essentially of dendrites, the name *dendron* was adopted.

Fig. 1B illustrates a typical spine synapse that makes an intimate contact with an apical dendrite of a pyramidal cell (Fig. 1; Fig. 3A and D). The ultrastructure of such a synapse has been intensively studied by Akert and his associates (14, 15). From the inner surface of a bouton confronting the synaptic cleft (d in Fig. 1B, the active site in Fig. 3A), dense projections in triangular array form the presynaptic vesicular grid (PVG) (Fig. 3A–E). Fig. 3B is a photomicrograph of a tangential section of a PVG showing the dense projections in triangular array with the faint synaptic vesicles fitting snugly in hexagonal array. The spherical synaptic vesicles, 50–60 Å in diameter, with their content of transmitter molecules, can be seen in the idealized drawings of the PVG (Fig. 3C and D) with the triangularly arranged dense projections, the active zone, and the hexagonal array of synaptic vesicles (14, 15). In a more primitive form the PVG can be seen in synapses of the fish Mauthner cell (17).

A nerve impulse propagating into a bouton causes a process called exocytosis. At most a nerve impulse evokes a single exocytosis from a PVG (Fig. 3D and G). This limitation is probably due to the vesicles being embedded in the paracrystalline PVG (Fig. 3B–E).

Exocytosis is the basic unitary activity of the cerebral cortex. Each all-or-nothing exocytosis of synaptic transmitter results in a brief excitatory postsynaptic depolarization (EPSP). Summation by electrotonic transmission of many hundreds of these milli-EPSPs is required for an EPSP large enough (10–20 mV) to generate the discharge of an impulse by a pyramidal cell. This impulse will travel along its axon (Fig. 2A) to make effective excitation at its many synapses. This is the conventional macro-operation of a pyramidal cell of the neocortex (Fig. 1) and it can be satisfactorily described by classical physics and neuroscience, even in the most complex design of network theory and neuronal group selection (10, 18, 19).

Exocytosis has been intensively studied in the mammalian central nervous system, where it is meanwhile possible to refine the study by utilizing a single excitatory impulse to generate EPSPs in single neurons that are being studied by intracellular recording. The initial studies were on the monosynaptic action on motoneurons by single impulses in the large Ia afferent fibres from muscle (20). More recently (21)

Abbreviations: EPSP, excitatory postsynaptic depolarization; PVG, presynaptic vesicular grid; SMA, supplementary motor area.

[‡]Approximate values can be given for the synaptic connectivity of an apical bundle. The input would be largely by the spine synapses (Figs. 1 and 2A), of which there would be over 5000 on a lamina V apical dendrite with its lateral branches and terminal tuft (Fig. 2A), but more usually there would be about 2000. If there are 70–100 apical dendrites in a bundle, the number of total spine synapses would be well over 100,000.

The publication costs of this article were defrayed in part by page charge payment. This article must therefore be hereby marked "advertisement" in accordance with 18 U.S.C. §1734 solely to indicate this fact.

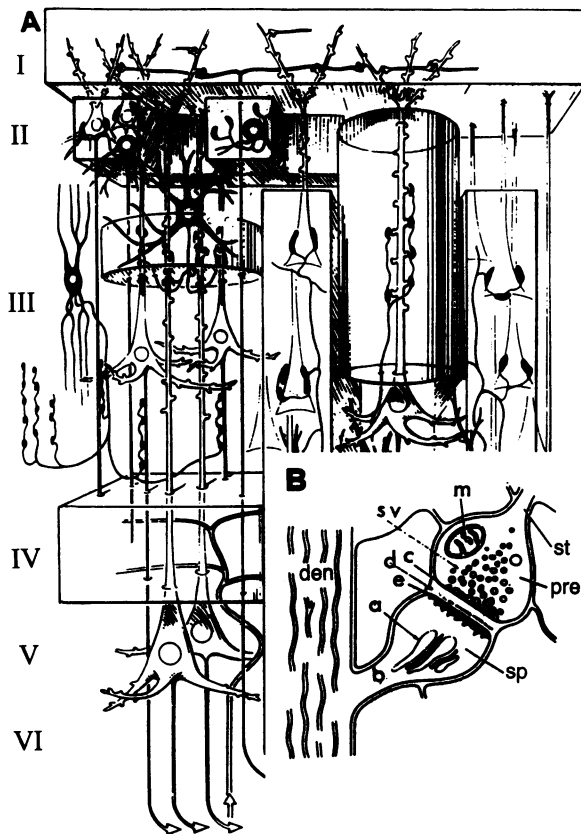


FIG. 1. (A) Three-dimensional construct by Szentagothai (10) showing cortical neurons of various types. (B) Detailed structure of a spine (sp) synapse on a dendrite (den); st, axon terminating in synaptic bouton or presynaptic terminal (pre); sv, synaptic vesicles; c, presynaptic vesicular grid (PVG in text); d, synaptic cleft; e, postsynaptic membrane; a, spine apparatus; b, spine stalk; m, mitochondrion (11).

it was found that the signal-to-noise ratio was much better for the neurons projecting up the dorso-spino-cerebellar tract (DSCT) to the cerebellum.

This successful quantal resolution for DSCT neurons and motoneurons gives confidence in the much more difficult analysis of neurons of the cerebral cortex, which provide the key structures of neural events that could be influenced by mental events. The signal-to-noise ratio was so low in the studies of CA1 neurons of the hippocampus that so far only three quantal analyses have been reliable in the complex deconvolution procedure.

In the most reliable analysis, a single axon of a CA3 hippocampal pyramidal cell set up an EPSP of quantal size $278 \mu\text{V}$ (mean value) in a single CA1 hippocampal pyramidal cell with approximately equal probabilities of release at each active site ($n = 5$) of 0.27 (22). In the alternative procedure the single CA3 impulse projecting to a CA1 pyramidal cell was directly stimulated in the stratum radiatum. The EPSPs delivered by the deconvolution analysis of two CA1 pyramidal cells were of quantal sizes $224 \mu\text{V}$ and $193 \mu\text{V}$ with probabilities ($n = 3$) of 0.24 and ($n = 6$) of 0.16, respectively (23). For a systematic review, see ref. 24.

Quantum Mechanical Model of Exocytosis

In the whole electrophysiological process of building up the summed EPSP experienced in the soma, there is only one element where quantal processes can play a role. When a bouton is activated by a nerve impulse, exocytosis occurs only with a certain probability, which is much less than 1. This calls for, in principle, the introduction of thermody-

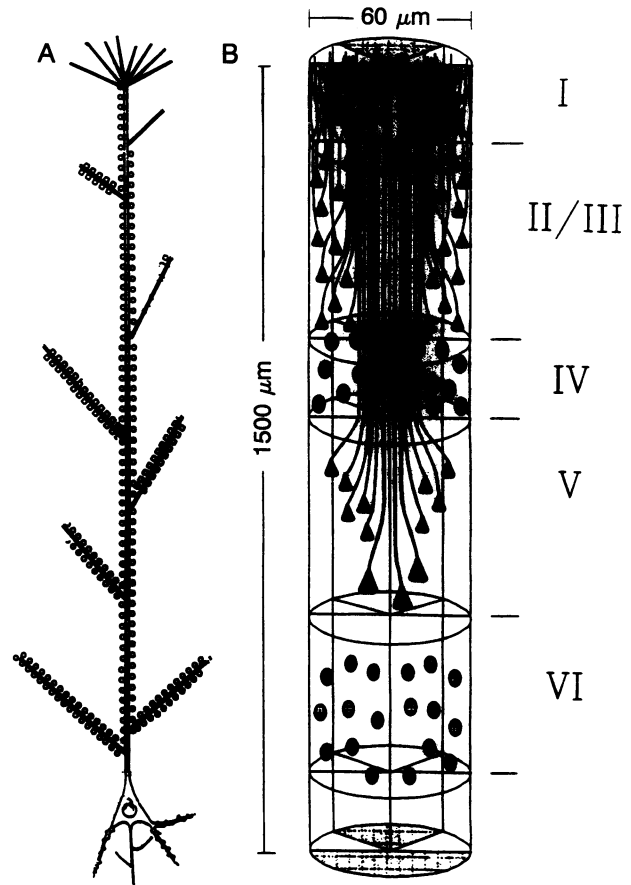


FIG. 2. (A) Drawing of a lamina V pyramidal cell with its apical dendrite showing the side branches and the terminal tuft, all studded with spine synapses (not all shown). The soma with its basal dendrites has an axon with axon collateral before leaving the cortex. (B) Drawing of the six laminae of the cerebral cortex with the apical dendrites of pyramidal cells of laminae II, III and V, showing the manner in which they bunch in ascending to lamina I, where they end in tufts (A. Peters, personal communication).

namic or quantum mechanical statistical concepts. We wish to make it clear that we adhere to the quantal standpoint. As has been pointed out (1, 2, 5), the conscious action of the brain could hardly be understood if the brain were in its entirety functioning on the basis of classical physics. Also, the relative constancy of the emission probability for single bouton release (21-24) can hardly be explained on the basis of thermal fluctuations.

Because the resulting EPSP is the *independent statistical sum* of several thousands of local EPSPs at spine synapses on each dendrite (Fig. 2A), we can concentrate on the process of exocytosis at each individual bouton.

Exocytosis is the opening of a channel in the PVG and discharge of the vesicle's transmitter molecules into the synaptic cleft (Fig. 3 F and G). It is, as a whole, certainly a classical membrane-mechanical process. To investigate further the possible role of quantum mechanics in the probabilistic discharge, one has to set up a model for the trigger mechanism by which Ca^{2+} prepares the vesicles of PVG for exocytosis.

For this purpose we adopt the following concept: preparation for exocytosis means bringing the paracrystalline PVG into a metastable state from which exocytosis can occur. The trigger mechanism is then modeled by the motion of a quasiparticle with 1 degree of freedom along a collective coordinate, and over an activation barrier (Fig. 4). This motion sets in by a quantum mechanical tunneling process through the barrier (similar to radioactive decay).

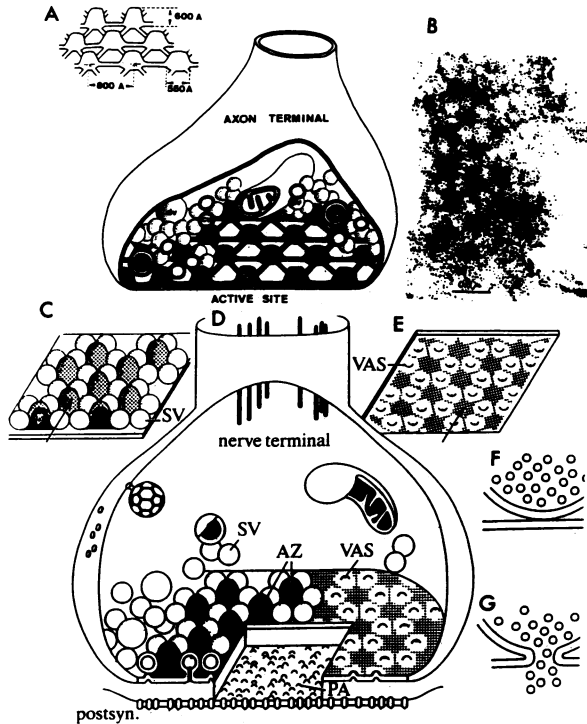


FIG. 3. (A) Axon terminal, or bouton, showing dense projections (dp) projecting from the active site with cross linkages forming the PVG, which is drawn in the *Inset* with dimensions (14). cv, small vesicle; dv, big vesicle. (B) Tangential section through the presynaptic area. A section of the patterns of dense projections and synaptic vesicles, triangular and hexagonal, of the PVG is clearly represented. (Bar = 0.1 μm .) [Reprinted from ref. 15 with permission.] (C–E) Active zone (AZ) of mammalian central synapse showing geometrical design (11). SV, synaptic vesicle; VAS, vesicle attachment site; PA, presynaptic area. (F) Synaptic vesicle in apposition. (G) Exocytosis (16).

The situation is determined by two characteristic energies: (i) the thermal energy, E_{th} , which the quasiparticle adopts in a thermal surrounding of temperature T . It is for our quasiparticle with 1 degree of freedom given by

$$E_{\text{th}} = \frac{1}{2} k_B T, \quad [1]$$

where k_B is the Boltzmann constant; (ii) the quantum mechanical zero-point energy, E_0 , of a particle of mass M localized over a distance of Δq . It follows from Heisenberg's uncertainty relation $\Delta p \cdot \Delta q \approx 2\pi\hbar$. If we adopt the lower limit (this would correspond to the ground state in a confining potential well), we obtain

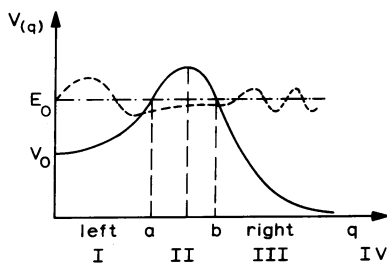


FIG. 4. The collective potential, $V(q)$, for the motion of the quasiparticle of energy E_0 which triggers exocytosis. The dashed curve sketches a tunneling state through the barrier. At the beginning the wave packet is located in the left area. After time τ the amplitude has a part left of the barrier and a part right of the barrier.

$$E_0 = \frac{(\Delta p)^2}{2M} = \left(\frac{2\pi\hbar}{\Delta q} \right)^2 \frac{1}{2M}. \quad [2]$$

We can define a borderline between the quantal and the classical regime by putting $E_0 = E_{\text{th}}$. $E_0 \gg E_{\text{th}}$ is then the quantal, and $E_{\text{th}} \gg E_0$ the thermal regime.

For fixed T and Δq the borderline equality determines a critical mass, M_c , for the quasiparticle. Dynamic processes which involve quasiparticle masses much larger than M_c belong to the classical regime, whereas for $M \ll M_c$ we are in the quantal regime. Taking $T = 300$ K and $\Delta q \approx 1$ \AA , we obtain $M_c \approx 10^{-23}$ g $\approx 6 M_H$, with M_H being the mass of a hydrogen atom.

This estimate shows quite clearly that a quantum mechanical trigger for exocytosis must reside in an atomic process—e.g., the movement of a hydrogen bridge by electronic rearrangement.

To make the model quantitative, we attribute to the triggering process of exocytosis a continuous collective variable, q , for the quasiparticle. The motion is characterized by a potential energy, $V(q)$, which may take on a positive value at stage I (Fig. 4), according to the metastable situation before exocytosis, then rises toward a maximum at stage II, and finally drops to zero (the arbitrary normalization) at stage IV. Fig. 4 gives a qualitative sketch of this potential barrier.

The time-dependent process of exocytosis is described by the one-dimensional Schrödinger equation for the wave function $\psi(q; t)$,

$$i\hbar \frac{\partial}{\partial t} \psi(q; t) = -\frac{\hbar^2}{2M} \frac{\partial^2}{\partial q^2} \psi(q; t) + V(q) \cdot \psi(q; t). \quad [3]$$

The initial condition for $t = 0$ (stage I, beginning of exocytosis) is a wave packet to the left of the potential barrier (Fig. 4).

The solution of Eq. 3 gives the wave function after time t , which consists of part of the wave packet still residing to the left of the barrier while another part has penetrated into the space to the right (see Fig. 4). The quantities

$$p_1(t) = \int_{\text{left}} \psi^*(q; t) \psi(q; t) dq$$

$$p_2(t) = \int_{\text{right}} \psi^*(q; t) \psi(q; t) dq \quad [4]$$

are the time-dependent probabilities that exocytosis will not occur (p_1) or that exocytosis will occur (by action of the trigger) (p_2). Of course, from normalization, $p_1(t) + p_2(t) = 1$.

The relevant time τ has to be defined as the duration of the quasistable situation in the paracrystalline PVG, after which the metastable state changes into a stable one where no exocytosis is possible. In our model this can be visualized as a dropping of the potential left of the barrier to a value for which barrier penetration has vanishingly small probability.

An approximate solution of the barrier penetration problem can be obtained from the Wentzel–Kramers–Brillouin (WKB) method (25). According to it the transmission coefficient T of a particle of mass M and energy E through the barrier is given by

$$T = \exp \left\{ -2 \int_a^b \frac{\sqrt{2M[V(q) - E]}}{\hbar} dq \right\}, \quad [5]$$

where a and b denote the classical turning points for the motion left and right of the barrier (Fig. 4). The probability

per unit time for penetration of the barrier, w , can be obtained by the number of attempts that the particle undertakes to reach the barrier, ω_0 , times the barrier transmission coefficient, T ,

$$w = \frac{dp}{dt} = \omega_0 T, \quad [6]$$

with $\hbar\omega_0 = E_0$ by an appeal to Bohr's correspondence principle. Combining this with the general considerations formulated after Eq. 4, we obtain

$$p_2(\tau) = \tau \cdot \omega = \tau \cdot \omega_0 T. \quad [7]$$

At this stage we can estimate some numbers. Let us assume that the energy $E = E_0$ of the initial state (the wave packet localized to the left of the barrier) is the zero-point energy of a wave packet localized over the dimension of the atomic site of the trigger, which we estimate roughly to be $\Delta q \approx 1 \text{ \AA}$, and let us take for the mass M of our quasiparticle the mass of one hydrogen atom, $M = 1.7 \times 10^{-24} \text{ g}$. Then we obtain, using Eq. 2, $E_0 \approx 8.3 \times 10^{-2} \text{ eV}$. This leads to a frequency, from $E_0 = \hbar\omega_0$, of $\omega_0 \approx 1.3 \times 10^{14} \text{ s}^{-1}$. Estimating τ , the time of the metastable instability, to be of the order of electronic transition processes which is $\tau \approx 10^{-13} - 10^{-14} \text{ s}$ we obtain from Eq. 7 $p_2(\tau) \sim 10 \cdot T$ to $100 \cdot T$. With the observed p_2 of about 0.25, this gives for the barrier penetration factor T the reasonable span of 4×10^{-2} to 4×10^{-3} .

Up to now we have based our model considerations on the release of one single vesicle located in the vesicular grid of the bouton. There are about 40 vesicles altogether in this paracrystalline structure, but never does more than one vesicle emit transmitter molecules into the synaptic cleft after stimulation by a nerve impulse. This certainly means that the vesicles in the vesicular grid do not act independently, but rather that *immediately* after one vesicle is triggered for releasing its content the interaction between them blocks further exocytosis. The paracrystalline structure of the PVG makes it possible to have long-range interactions between the constituents, as is well known from ordered quantum systems. According to our numerical estimates, the relaxation time for the blocking process is of the order of femtoseconds.

With this observation we can discuss the many-body aspect of exocytosis from the vesicular grid. To this end we attribute schematically to each vesicle in the grid two states, ψ_0 and ψ_1 , where ψ_0 is the state before and ψ_1 the state after exocytosis has been triggered. We can safely assume that the different vesicles are so well separated that we can treat them as distinguishable particles. The wave function of N vesicles is then a product of denumerable states,

$$\Psi(1, \dots, N) = \psi_{i_1}^{(1)} \cdot \psi_{i_2}^{(2)} \dots \psi_{i_N}^{(N)}; \quad i_j = \{0, 1\}. \quad [8]$$

Before exocytosis the wave function has the form

$$\Psi_0(1, \dots, N) = \psi_0^{(1)} \dots \psi_0^{(N)}. \quad [9]$$

The observation that in response to a presynaptic impulse only one vesicle can empty its transmitter molecules into the synaptic cleft leads to a properly normalized wave function after the trigger for exocytosis has functioned of the form

$$\Psi_1(1, \dots, N) = \frac{1}{\sqrt{N}} [\psi_1^{(1)} \cdot \psi_0^{(2)} \dots \psi_0^{(N)} + \psi_0^{(1)} \cdot \psi_1^{(2)} \cdot \psi_0^{(3)} \dots \psi_0^{(N)} + \dots + \psi_0^{(1)} \dots \psi_0^{(N-1)} \cdot \psi_1^{(N)}]. \quad [10]$$

All other states are pushed up in energy by the long-range interaction so far that they cannot be excited by the nerve impulse.

Calculating the probability for exocytosis from the N -body wave functions, Eqs. 9 and 10, one obtains the same result as was obtained from the barrier-penetration problem of one vesicle, since the trigger can change the state of only one vesicle, but there are N such possibilities. This leads to the observable consequence that the probability for exocytosis of one bouton does not depend on the number of identical vesicles occupying the PVG.

Our model introduces into the activity of the neocortex a quantum probabilistic aspect that leads to a selection of choices according to a quantum probability amplitude.

Generation of Neural Events by Mental Events

Ingvar (26) introduced the term "pure ideation," which is defined as cognitive events that are unrelated to any ongoing sensory stimulation or motor performances. He and associates at the University of Lund introduced the study of the regional cerebral blood flow to display by cerebral ideography the activity of the brain in pure ideation in all the immense variety generated by the psyche. By radioxenon mapping Roland *et al.* (27) demonstrated that in pure motor ideation of complex hand movements there was activation of the supplementary motor area (SMA) on both sides. By the more accurate technique of positron emission tomography (PET) scanning Raichle and his associates (28) demonstrated a widespread patchy activity of the neocortex during specific mental operations in selective attention.

In a complementary procedure, averaging techniques have been used to record the electrical fields generated by the brain (centered on the SMA) in the willing of a movement, the so-called readiness potential (29). In exquisitely designed experiments Libet (30) has discovered that in conscious willing there is a cerebral activation about 200 ms before the movement (see ref. 30, *General Discussion*).

Intracellular recording from a cortical neuron, a hippocampal pyramidal cell, discloses a continuous intense activity which can be interpreted as milli-EPSPs generated by the continuous synaptic bombardment with exocytoses by the thousands of boutons on its dendrites (Fig. 2A). Deconvolution analysis has shown that an impulse invading a bouton (Fig. 3 A and D) evokes an exocytosis and a milli-EPSP with a probability of about 0.2–0.3 (22, 23).

Combining these observations with our quantum mechanical analysis of bouton exocytosis, we present now the hypothesis that the mental intention (the volition) becomes neurally effective by *momentarily increasing the probability of exocytosis* in selected cortical areas such as the SMA neurons (31). In the language of quantum mechanics this means a *selection of events* (the event that the trigger mechanism has functioned, which is already prepared with a certain probability; cf. Fig. 4 and Eq. 4). This act of selection is related to Wigner's selection process of the mind on quantal states (6), and its mechanism clearly lies beyond ordinary quantum mechanics. Effectively this selection mechanism increases the probability for exocytosis, and in this way generates increased EPSPs *without violation of the conservation laws*. Furthermore, the interaction of mental events with the quantum probability amplitudes for exocytosis introduces a coherent coupling of a large number of individual amplitudes of the hundreds of thousands of boutons in a dendron. This then leads to an overwhelming variety of actualities, or modes, in brain activity. Physicists will realize the close analogy to laser-action, or, more generally, to the phenomenon of self-organization.

Beyond that micro-stage the volition would operate as explained by neuroscience in the conventional manner.

There could be summation of the milli-EPSPs generated by the thousands of boutons on each pyramidal cell (Fig. 2A), and then the hundred or so pyramidal cells of a dendron (Fig. 2B) would interact in generating the ongoing discharge of the SMA neurons (31), and further to the motor pyramidal cells with discharges down the pyramidal tract to the motoneurons. The resulting impulse discharges in motor nerves would effect the intended movement with all the control systems cooperating.

Voluntary movement has been explained in principle. This explanation can be extended to the action of all mental influences on the brain—for example, in carrying out any planned action, such as speech.

Conclusions

Based on a careful analysis of neocortical activity, we argue that exocytosis is its key mechanism. Exocytosis, the momentary opening of a channel in the presynaptic membrane of a bouton with liberation of the transmitter substance (Fig. 3 F and G), is caused by a nerve impulse. As has been established in many experiments (22–24), exocytosis is an all-or-nothing-event, occurring with probabilities of the order of 0.25. This observation led us to set up a quantum mechanical model for the trigger mechanism of exocytosis, based on the tunneling of a quasiparticle representing the trigger.

The quantum treatment of exocytosis links the neocortical activity with the existence of a large number of quantum probability amplitudes, since there are more than 100,000 boutons in a bundle of dendrites called a dendron (Fig. 2 A and B). In the absence of mental activity these probability amplitudes act independently, causing fluctuating EPSPs in the pyramidal cell. We put forward the hypothesis that mental intention becomes neurally effective by momentarily increasing the probabilities for exocytoses in a whole dendron (Fig. 2B) and, in this way, couples the large number of probability amplitudes to produce coherent action.

Our hypothesis offers a natural explanation for voluntary movements caused by mental intentions without violating physical conservation laws. It has been shown experimentally that intentions activate the cerebral cortex in certain well-defined regions prior to the movement (26–28).

The unitary hypothesis transforms the manner of operation of the intention. One has to recognize that, in a lifetime of learning, the intention to carry out a particular movement would be directed to those particular dendrons of the neocortex that are appropriate for bringing about the required actions. We believe that the proposed hypothesis accounts for action across the mind–brain interface.

We acknowledge the help of Dr. Stephen Redman in calculations of probabilities of release.

1. Stapp, H. P. (1991) *Found. Physics* **21**, 1451–1477.
2. Squires, E. J. (1988) *Found. Physics Lett.* **1**, 13–20.
3. Donald, M. J. (1990) *Proc. R. Soc. London A* **424**, 43–93.
4. Margenau, H. (1984) *The Miracle of Existence* (Ox Bow, Woodbridge, CT).
5. Eccles, J. C. (1990) *Proc. R. Soc. London B* **240**, 433–451.
6. Wigner, E. P. (1967) in *Symmetries and Reflections* (Indiana Univ. Press, Bloomington, IN), pp. 153–184.
7. von Neumann, J. (1955) *Mathematical Foundations of Quantum Mechanics* (Princeton Univ. Press, Princeton).
8. Everett, H. (1957) *Rev. Mod. Phys.* **29**, 454–462.
9. Popper, K. & Eccles, J. C. (1977) *The Self and Its Brain* (Springer, Berlin).
10. Szentagothai, J. (1978) *Proc. R. Soc. London B* **201**, 219–248.
11. Gray, E. G. (1982) *Trends Neurosci.* **5**, 5–6.
12. Peters, A. & Kara, D. A. (1987) *J. Comp. Neurol.* **260**, 573–590.
13. Schmolke, C. & Fleischhauer, K. (1984) *Anat. Embryol.* **169**, 125–132.
14. Pfenninger, K., Sandri, C., Akert, K. & Eugster, C. H. (1969) *Brain Res.* **12**, 10–18.
15. Akert, K., Peper, K. & Sandri, C. (1975) in *Cholinergic Mechanisms*, ed. Waser, P. G. (Raven, New York), pp. 43–57.
16. Kelly, R. B., Deutsch, J. W., Carlson, S. S. & Wagner, J. A. (1979) *Annu. Rev. Neurosci.* **2**, 399–446.
17. Korn, H. & Faber, D. S. (1987) in *New Insights into Synaptic Function*, eds. Edelman, G. M., Gall, W. E. & Cowan, W. M. (Wiley, New York), pp. 57–108.
18. Mountcastle, V. B. (1978) in *The Mindful Brain*, ed. Schmitt, F. C. (MIT Press, Cambridge, MA), pp. 7–50.
19. Edelman, G. M. (1989) *The Remembered Present: A Biological Theory of Consciousness* (Basic Books, New York).
20. Jack, J. J. B., Redman, S. J. & Wong, K. (1981) *J. Physiol. (London)* **321**, 65–96.
21. Walmsley, B., Edwards, F. R. & Tracey, D. J. (1987) *J. Neurosci.* **7**, 1037–1046.
22. Sayer, R. J., Friedlander, M. J. & Redman, S. J. (1990) *J. Neurosci.* **10**, 626–636.
23. Sayer, R. J., Redman, S. J. & Andersen, P. (1989) *J. Neurosci.* **9**, 845–850.
24. Redman, S. J. (1990) *Physiol. Rev.* **70**, 165–198.
25. Messiah, A. (1961) in *Quantum Mechanics* (North-Holland, Amsterdam), pp. 231–242.
26. Ingvar, D. H. (1990) in *The Principles of Design and Operation of the Brain*, eds. Eccles, J. C. & Creutzfeld, O. (Springer, Berlin), pp. 433–453.
27. Roland, P. E., Larsen, B., Lassen, N. A. & Skinhøj, E. (1980) *J. Neurophysiol.* **43**, 118–136.
28. Posner, M. I., Petersen, S. E., Fox, P. T. & Raichle, M. E. (1988) *Science* **240**, 1627–1631.
29. Deecke, L. & Lang, V. (1990) in *The Principles of Design and Operation of the Brain*, eds. Eccles, J. C. & Creutzfeld, O. (Springer, Berlin), pp. 303–341.
30. Libet, B. (1990) in *The Principles of Design and Operation of the Brain*, eds. Eccles, J. C. & Creutzfeld, O. (Springer, Berlin), pp. 185–205 plus General Discussion, pp. 207–211.
31. Eccles, J. C. (1982) *Arch. Psychiatr. Nervenkrank.* **231**, 423–441.